Relationship between dermal birefringence and the skin surface roughness of photoaged human skin

Shingo Sakai
Noriaki Nakagawa
Kanebo Cosmetics, Inc.
Basic Research Laboratory
5-3-28, Kotobuki
Odawara, Kanagawa 250-0002
Japan

Masahiro Yamanari
Arata Miyazawa
Yoshiaki Yasuno
University of Tsukuba
Computational Optics Group
Tennodai 1-1-1
Tsukuba, Ibaraki 305-8573
Japan

Masayuki Matsumoto
Kanebo Cosmetics, Inc.
Products Science Research Laboratory
Kotobuki 5-3-28
Odawara, Kanagawa 250-0002
Japan

Abstract. The dermal degeneration accompanying photoaging is considered to promote skin roughness features such as wrinkles. Our previous study demonstrated that polarization-sensitive spectral domain optical coherence tomography (PS-SD-OCT) enabled noninvasive three-dimensional evaluation of the dermal degeneration of photoaged skin as a change in dermal birefringence, mainly due to collagenous structures. Our purpose is to examine the relationship between dermal birefringence and elasticity and the skin morphology in the eye corner area using PS-SD-OCT. Nineteen healthy male subjects in their seventees were recruited as subjects. A transverse dermal birefringence map, automatically produced by the algorithm, did not show localized changes in the dermal birefringence in the part of the main horizontal wrinkle. The averaged upper dermal birefringence, however, showed depth-dependent correlation with the parameters of skin roughness significantly, suggesting that solar elastosis is a major factor for the progress of wrinkles. Age-dependent parameters of skin elasticity measured with Cutometer did not correlate with the parameters. These results suggest that the analysis of dermal birefringence using PS-SD-OCT enables the evaluation of photoaging-dependent upper dermal degeneration related to the change of skin roughness. © 2009 Society of Photo-Optical Instrumentation Engineers. [DOI: 10.1117/1.3207142]

Keywords: polarization-sensitive optical coherence tomography; birefringence; skin; collagen; solar elastosis; photoaging; wrinkles; surface roughness; elasticity.

Paper 08407RR received Nov. 15, 2008; revised manuscript received Jun. 22, 2009; accepted for publication Jun. 23, 2009; published online Aug. 25, 2009.

1 Introduction

Aging brings changes in skin morphology such as microrelief and wrinkles.[1–3] Particularly, the deep wrinkles in exposed areas such as the back of the neck and the face are an issue not only in cosmetic science but also in dermatology. Aging in the exposed areas is called photoaging, or extrinsic aging, which is different from intrinsic aging. Photoaged skin shows histological alternation, such as the Grenz zone and solar elastosis.[4–6] In general, the upper dermis is roughly made up of two layers, i.e., the papillary dermis and reticular dermis.[7] The papillary dermis is a fine-collagen layer with a thickness of about 100 μm.[7–9] The reticular dermis is a thick layer of collagen bundles located just under the papillary dermis.[8] As solar elastosis (accumulative degeneration of elastic fibers) progresses in the course of photoaging, the degenerated elastic fibers come to occupy most of the reticular dermis, and the papillary dermis tends to be clear. This clear layer of papillary dermis is called the Grenz zone.[4,10] Photoaged skin demonstrates decreased collagen content,[10–13] and disorganized collagen fibers[14–16] have been observed under the epidermis. Oxytalan fiber also decreases in this region.[17] Solar elastosis, which does not have birefringence, shows characteristic deposition of abnormal elastin under the Grenz zone. Characteristic depth-dependent dermal degeneration progresses with photoaged skin. However, there are not many reports regarding the relationship between the histological dermal degeneration and the morphology of wrinkles. Kligman et al.[18] and Bosset et al.[19] reported that wrinkles did not have any diagnostic histological changes, compared with the surrounding sites. Tsuji et al.[20,21] demonstrated the progression of solar elastosis accompanying wrinkle formation. Contet-Audonneau et al.[22] showed the immunohistochemical changes of the differentiational markers such as filaggrin and transglutaminase of keratinocytes and collagen IV and elastic fibers at the epidermal–dermal junction in the bottom of wrinkles. Significantly, the deformation of the skin by physical contact during biopsy procedures makes it very difficult to observe the histology of wrinkles with high precision.

Alternatively, chronic exposure to ultraviolet rays has been shown to promote wrinkle formation in animal models. The degeneration of collagen,[23] elastin,[24] basal membrane,[25] and keratin,[26] are proposed as candidates for wrinkle-formation factors. It is very important to identify and quantify the structural change directly related to the morphology of wrinkles. The measurement of skin elasticity is thought to be helpful in the evaluation of structural change through photoaging. Skin elasticity decreases with aging.[27–29] Examinations using sub-

Address all correspondence to: Shingo Sakai, Basic Research Laboratory, Kanebo Cosmetics, Inc., 5-3-28, Kotobuki, Odawara, Kanagawa, 250-0002, Japan. Tel: +81-465-34-6116; Fax: +81-465-34-3037; E-mail: sakai.shingo@kanebocos.co.jp

jects of all generations demonstrate a significant correlation between the morphology parameters of wrinkles and skin elasticity.[30–32] The elasticity of sun-exposed skin decreases more than that of nonexposed skin in aging.[44,29,33,34] However, little statistical analysis for the relationship between skin elasticity and skin roughness such as wrinkles using subjects of the same generation has been reported. So far, we cannot sufficiently understand the quantified dermal degeneration directly related to wrinkle morphology by measurement of skin elasticity. Alternatively, ultrasonic imaging is also useful for the evaluation of the dermal structure.[34–37] De Rigal et al. reported the evaluation of the dermal degeneration as upper dermal echogenicity using ultrasonic imaging.[34,35] They demonstrated that the subepidermal nonechogenic band increased in the dorsal forearm (exposed site) more than in the ventral one (nonexposed site) of the older subjects. None of the earlier studies, however, have statistically examined the relationship between dermal echogenic and objective skin roughness of the eye-corner area in subjects of the same age group.

Polarization-sensitive optical coherence tomography (PS-OCT) has higher resolution than ultrasonic imaging and can visualize not only the backscatter light intensity, but also dermal birefringence related to collagenous structures in biological tissue. To take advantage of these capabilities, PS-OCT has been applied to dermatology in several earlier studies.[38,39] PS-OCT analyses of dermal birefringence have been reported in cases of scars, burns, and wound-healing with changes of the collagenous structure of the skin.[38,40–42] Fiber-based polarization-sensitive spectral domain optical coherence tomography (PS-SD-OCT) using B-scan-oriented polarization modulation was developed for high speed and highly sensitive measurement.[43] PS-SD-OCT enables three-dimensional (3-D) analysis of the dermal birefringence, which produces a transverse birefringence map corresponding to the surface morphology of the skin. Moreover, noninvasive and noncontact measurement of dermal birefringence by PS-SD-OCT is expected to be useful for wrinkle evaluation, because wrinkles are deformed easily by external force and biopsy methods. In our previous study, we demonstrated upper dermal degeneration by photoaging but not intrinsic aging as changes in dermal birefringence using PS-SD-OCT[44]. In this study, we have used PS-SD-OCT to three-dimensionally analyze the dermal birefringence in the eye-corner area including a horizontal main wrinkle of subjects in their seventies, measured the skin elasticity and morphology of the same area, and examined the relationship between them.

2 Materials and Methods

2.1 Subjects

Nineteen healthy, elderly male Japanese volunteers were recruited. The volunteers were selected within a narrow age range (71.8 ± 2.3 years old, mean ± standard deviation) to eliminate the effects of intrinsic aging in this study. All of the subjects gave their informed consent to participate. The protocol was conducted according to the Declaration of Helsinki Principles and approved by the ethics committees of Kanebo Cosmetics, Inc., and the University of Tsukuba. The subjects washed their faces with a facial wash and tap water and their vellus hair around the eye-corner area was shaved using an electric shaver. The areas (6 mm × 3 mm) of the eye corner,
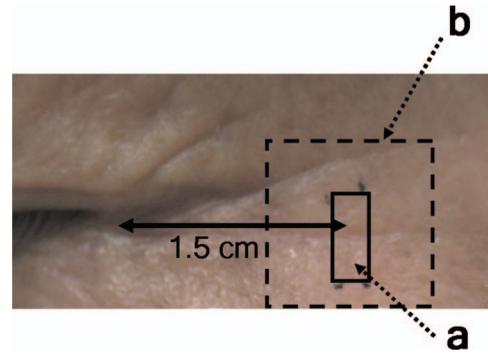

Fig. 1 Targets for the measurements. Area *a* (6 mm × 3 mm) was analyzed for dermal birefringence and skin elasticity. Areas *a* and *b* (1.8 cm × 1.3 cm) were analyzed for the depth and volume of the wrinkle by Voxelan and for the roughness by Primos using replicas, respectively.

keeping the distance to the outer corner of the eyes (1.5 cm) of each subject, were sequentially measured using PS-SD-OCT and imaged using a CCD camera (Fig. 1) in a room at a constant temperature of 25 °C (humidity, 50% Rh). After measuring dermal birefringence, negative replicas (25 mm × 25 mm) of the areas including the areas scanned by PS-SD-OCT were taken by using SILFLO (Flexico Developments Ltd., England). Skin elasticity at the scanned areas was measured by Cutometer SEM 574 (Courage and Khazaka, Köln, Germany) at 15 min after taking replicas. Probe diameter and suction were 2 mm and 350 mbar, respectively. The time-strain curve was recorded by sucking up a section of skin for 3 s (350 mbar) and then releasing the skin for 3 s. Ue and Uv are the immediate deformation at 0.1 s after commencing the sucking-up and delayed deformation, respectively. Uf and Ur are max deformation and immediate restoration at 0.1 s after release, respectively. Uv/Ue and Ur/Uf were determined as described by Cua et al.[15,28].

2.2 PS-SD-OCT System

The PS-SD-OCT system was described in previous reports.[44,43] The light source was a superluminescent diode (SLD-37-HP, Superlum, Moscow, Russia) with a central wavelength of 840 nm, a bandwidth of 50 nm, and a depth resolution of 8.3 μm in air (Fig. 2). After the polarization was vertically aligned by a linear polarizer (LP), an electro-optic (EO) modulator with a fast axis of 45 deg modulated the incident polarization state. The incident beam was coupled into
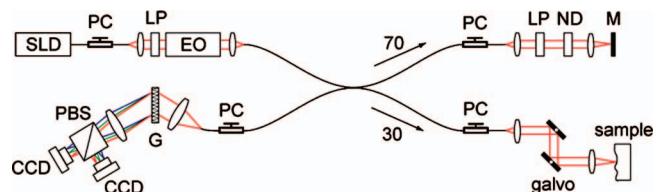
Fig. 2 Diagram of the PS-SD-OCT system. The following notations are used: SLD, superluminescent diode; PC, polarization controller; ND, neutral density filter; LP, linear polarizer; EO, electro-optic modulator; M, mirror; G, grating; PBS, polarizing beamsplitter; CCD, line-CCD camera.

a fiber coupler, the splitting ratio of which is 70/30. The LP in the reference arm provided constant amplitude and constant relative phase between the two orthogonal polarizations at the spectrometer, independent of the incident state of the polarization. In the sample arm, the beam was scanned by the two-axis galvano scanner mirror. The probing power was 700 μW, which is below the safe occupational exposure level established by the American National Standards Institute (ANSI Z 136.1). The backscattered signal from the skin was coupled into the fiber again and detected by the polarization-sensitive spectrometer. The spectrometer contained a polarizing beamsplitter and two line-scan CCD cameras for the simultaneous detection of the horizontal and vertical polarization channels. The line trigger for both cameras (27.7 kHz) was synchronized with the EO modulator. The sensitivity was 100.7 dB. The targeted area on the skin was 6 mm $\times$ 3.0 mm, which corresponds to 2045 pixels $\times$ 70 pixels. The measurement time was 5.5 s.

2.3 Algorithm for Analysis of Dermal Birefringence

The three-dimensional (3-D) distributions of backscattering intensity and double-pass phase retardation in the sample were measured using a method of B-scan-oriented polarization modulation, as described in the previous study.[43] The birefringence of the sample is represented by the slope of the measured phase retardation, a parameter that shows the cumulative effect of birefringence along the depth. This same parameter, the slope of phase retardation, has been regarded as an essential quantitative index of the dermal collagen state.[39–41] To analyze the histological-change-based characteristic of dermal birefringence in this study, two fixed-depth ranges (100 to 200 μm and 200 to 300 μm from the skin surface) were applied for the slope of the phase retardation. For each A-scan, double-pass phase retardation was moving-averaged by 30 axial pixels (30 pixels correspond to 93.5 μm). The surface of the sample was detected by thresholding the backscattering intensity image. Pixels above the surface were removed, and the phase retardation data were realigned with respect to the surface. The slope of the phase retardation was calculated by applying the linear-regression fitting method to the fixed range. The moving average and the linear regression effectively suppressed low signal-to-noise-ratio points caused by the speckle noise. This procedure was used for each of the 70 B-scans, resulting in the two transverse slope maps, i.e., transverse birefringence maps 1 and 2 (1: 100- 200-μm depth region; 2: 200- 300-μm depth region). The averaged dermal birefringence 1 and 2 (ADB1 and ADB2) were determined by averaging the 2-D slope data of transverse birefringence maps 1 and 2, respectively (Fig. 3).

3 The Morphological Parameters of Wrinkles

3.1 Evaluation for Volume and Averaged Depth of Main Horizontal Wrinkle in Scanned Area

The replicas were performed by using a small object type 3-D surface morphology measurement system (Voxelan HEV-50S, Hamano Engineering Co., Ltd., Kawasaki, Japan).[29] This commercial system employed a noncontact morphological measurement method using laser slit beam and CCD cameras.
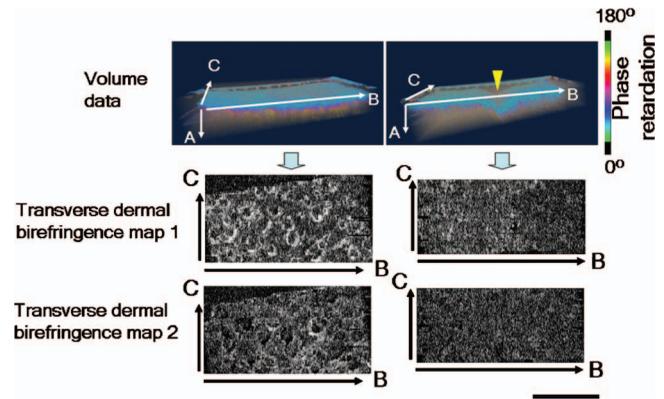

Fig. 3 Methods for producing the transverse dermal birefringence maps. A, B, and C indicate the direction of scan. Transverse birefringence map 1 and map 2 were produced by mapping the slope of phase retardation in each A-scan at the region of 100 to 200 μm and 200 to 300 μm from the surface two-dimensionally, respectively. Scale bar: 3 mm.

The measurable area was 10 mm $\times$ 9.4 mm. The accuracy of this system on the z axis is approximately 0.01 mm. The 3-D data obtained were analyzed using 3D-Rugle for Windows (Medic Engineering, Inc., Japan) The data obtained were subjected to corrective processing (e.g., flattening out of overall sloping and undulation and removal of low-level noise). The analysis data was generated by subtracting the third-order regression plane from the original data. After correction of the slope, the volume and the average depth of the main horizontal wrinkle in the ROI (6 mm $\times$ 3 mm), which was identical to the PS-SD-OCT measurement area, were calculated.

3.2 Evaluation for Skin Roughness of Replicas Using Primos

Measurements were carried out using the Primos system (GFMesstechnik GmbH, Berlin) for the 3-D analysis.[45,46] This commercial system is based on the so-called digital stripe projection technique, which is used as an optical measurement process. A parallel stripe pattern is projected onto the skin surface and depicted on the CCD chip for recording. The measuring field was 18 mm $\times$ 13 mm in the silicon replica, of which the PS-SD-OCT measurement area was located in the center. The length of the lines for calculating roughness parameters was 10 mm. The five lines were placed 2 mm apart in the center of the replicas. A wave undulation removal filter (polynomial filter, rank=5), which was in the Primos system software (Primos ver. 4.075), was used to remove the wave undulation of the obtained 3-D data. The acquisition software then made it possible to obtain 3-D measurements to determine roughness parameters of the skin. As roughness parameters, Ra, Rz, Sm and Wt were determined in this study. These parameters correspond to the German standardization norm DIN EN ISO 4288 and the international standardization ISO 4288 (1996). Ra is an arithmetic average value of profiles peaks within the total measuring length. Rz is the mean value of these different maxima obtained on five successive regions of the profile. Sm is the mean spacing between profiles peaks at the mean line measured over the assessment length. Wt is
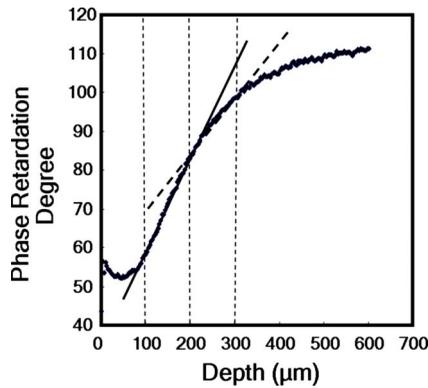
Fig. 4 A line depth profile of the phase retardation of the eye-corner area of a typical subject in his seventies. There were two regions having different birefringence in the dermis. Solid line: The automatically calculated slope of phase retardation at the 100 to 200-μm depth region from the skin surface (the dermal birefringence 1). Dashed line: The automatically calculated slope of phase retardation at the 200 to 300-μm depth region from the skin surface (the dermal birefringence 2).
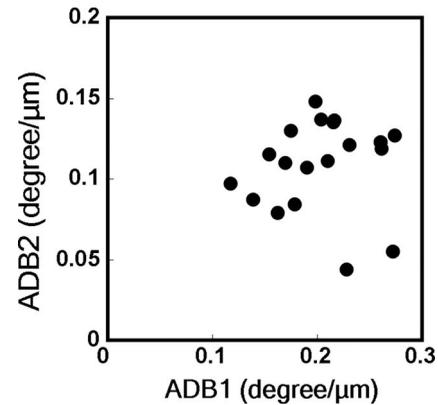
the vertical distance between the highest profile peak and the deepest profile valley of the waviness profile W within the measurement length.

Correlation analysis was examined using Pearson's correlation coefficients by statistical software, SPSS (SPSS ver. 12.0j, SPSS Japan, Inc., Tokyo).

4 Results

4.1 Individual Variation of Depth-Dependent Dermal Birefringence

We focused on depth-dependent change of the birefringence with dermal degeneration. Figure 4 shows a typical depth profile of phase retardation in an A-scan of a subject's eye-corner area. The averaging of phase retardation produced an offset at the surface. Since the measurable range of phase retardation is from 0 to pi, the phase noise around 0 retardation contributed only to the positive direction, as described in the previous study.[47] As reported,[39,41,44] the epidermis showed little change in phase retardation at the region of 0 to 100 μm from the surface. In our study, the dermal phase retardation was integrated with depth and saturated at depths deeper than 300 μm. Our phase retardation plots showed two distinctly different slopes. They were seen in all subjects (data not shown). The algorithm produced the transverse dermal birefringence maps 1 and 2, and calculated averaged dermal birefringence 1 (ADB1) and 2 (ADB2) of the two fixed-depth regions, 100 to 200 μm and 200 to 300 μm from the skin surface, respectively. In earlier studies, ADB1 mostly corresponded to the birefringence of the papillary dermis,[7,9] while ADB2 mostly corresponded to the birefringence of the upper reticular dermis, the layer where solar elastosis progresses. Some subjects showed higher ADB1 and lower ADB2 (Fig. 5), suggesting individual variations in depth-dependent dermal degeneration.

Fig. 5 Averaged dermal birefringence 1 (ADB1) did not correlate with averaged dermal birefringence 2 (ADB2) significantly. Nineteen subjects in their seventies were recruited.

4.2 Dermal Birefringence in the Parts of Wrinkles

To investigate the change of dermal birefringence localized in wrinkles, the transverse dermal birefringence maps were compared with images taken with a CCD camera. The averaged depth of the main horizontal wrinkles varied sufficiently from 80 μm to 820 μm (335 μm $\pm$ 214 μm). The horizontal wrinkles with significantly deep wrinkles (390 to 820 μm) did not have any pronounced localized changes of dermal birefringence (Fig. 6). The subject with the deepest wrinkle had an overall low intensity of transverse dermal birefringence map 2 (Fig. 6).
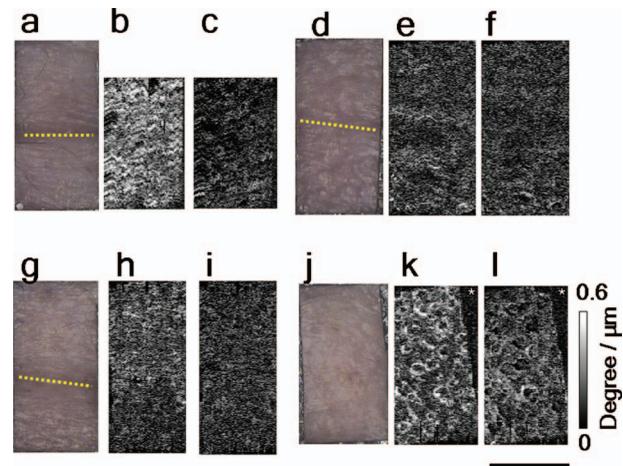
Fig. 6 Wrinkles did not have any localized changes of dermal birefringence. The eye corner areas of four subjects (a–c, d–f, g–i, j–l). (a), (g), (d), (j): Images of the CCD camera. (b), (h), (e), (k): Transverse dermal birefringence map 1 (100 to 200 μm). (c), (i), (f), (l): Transverse dermal birefringence map 2 (200 to 300 μm). Dotted line indicates valley of wrinkles: (a–i) deep wrinkles; (j–l) shallow wrinkles. Averaged depth of main wrinkle was 820 μm (a–c), 728 μm (d–f), 390 μm (g–i), 68 μm (j–l). Scale: 3 mm. (∗) The edge of window-type taped for marking.

Table 1 Averaged dermal birefringence (ADB) but not skin elasticity correlated with morphological parameters of skin surface.

Parameters		Birefringence		Cutometer	
		100 to 200 μm	200 to 300 μm	Uv/Ue	Ur/Uf
Voxelan (in the window)	Volume of the wrinkle	−0.270 (0.264)	−0.562 (0.012)	−0.011 (0.965)	−0.157 (0.522)
	Averaged depth of the wrinkle	−0.189 (0.439)	−0.537 (0.018)	−0.057 (0.817)	−0.098 (0.69)
Primos (in the large replica)	Ra	−0.293 (0.223)	−0.518 (0.023)	0.104 (0.671)	−0.22 (0.365)
	Rz	−0.093 (0.704)	−0.556 (0.014)	0.112 (0.647)	−0.279 (0.247)
	Sm	−0.543 (0.016)	−0.205 (0.400)	0.179 (0.463)	−0.089 (0.718)
	Wt	−0.573 (0.010)	−0.459 (0.048)	0.052 (0.833)	0.064 (0.795)

Note: $n=19$; values indicate correlation coefficient; ( ), p value.

4.3 Relationship between the Averaged Birefringence and Skin Roughness

The algorithm determined the averaged dermal birefringence (ADB1, ADB2) by each map. We compared them with morphological parameters of scanned areas by PS-SD-OCT and large areas including them using their replicas by Voxelan and Primos, respectively. ADB2 showed a significant negative correlation with the averaged depth ($r=-0.537$, $p=0.018$) and volume of the wrinkles ($r=-0.562$, $p=0.012$), parameters for the Voxelan measurements (Table 1). ADB1, however, did not show the correlation with them. ADB2 also showed a negative correlation with Ra ($r=-0.518$, $p=0.023$) and Rz ($r=-0.556$, $p=0.014$), roughness parameters of the large areas; however, ADB1 did not show any correlation with them (Tables 1 and 2; Fig. 7). ADB1 correlated with Sm ($r=-0.543$, $p=0.016$), a spacing parameter, significantly. Both ADBs showed a significant negative correlation with Wt, a waviness parameter (Tables 1 and 2; Fig. 7). These results suggested that the relationship between dermal degeneration and skin roughness was dependent on the depth.

4.4 Relationship between Skin Elasticity Measured by Cutometer and Skin Roughness

Neither Uv/Ue nor Ur/Uf, age-dependent parameters of skin viscoelasticity[28,29] correlated with any parameters of skin roughness significantly (Table 1; Fig. 8). They did not correlate with either averaged dermal birefringence significantly (data not shown).

5 Discussion

In this study, the correlation between upper dermal birefringence measured by the PS-SD-OCT system and skin roughness has been demonstrated. To our knowledge, this is previously unreported. Ra and Rz are thought to be objective roughness parameters for qualification of facial wrinkles.[30,46] Wt is also a major skin roughness parameter.[45,48] The Ra

Table 2 Averaged dermal birefringence (ADB) and skin roughness (Ra, Wt) of subject.

| Subject	ADB1 (deg/μm)	ADB1 (deg/μm)	Ra (μm)	Wt (μm)
1	0.272	0.055	58.7	225.5
2	0.175	0.130	25.0	143.8
3	0.162	0.079	14.2	84.2
4	0.228	0.044	45.5	171.1
5	0.274	0.127	13.7	52.8
6	0.216	0.136	29.0	81.9
7	0.204	0.137	38.2	144.5
8	0.139	0.087	42.7	289.7
9	0.190	0.107	20.4	73.7
10	0.210	0.111	51.3	185.6
11	0.216	0.136	31.3	131.6
12	0.178	0.084	48.1	224.5
13	0.117	0.097	66.9	385.2
14	0.169	0.110	45.8	151.6
15	0.231	0.121	29.2	114.5
16	0.261	0.119	24.0	102.7
17	0.198	0.148	15.7	64.6
18	0.154	0.115	33.6	224.9
19	0.260	0.123	21.0	83.8
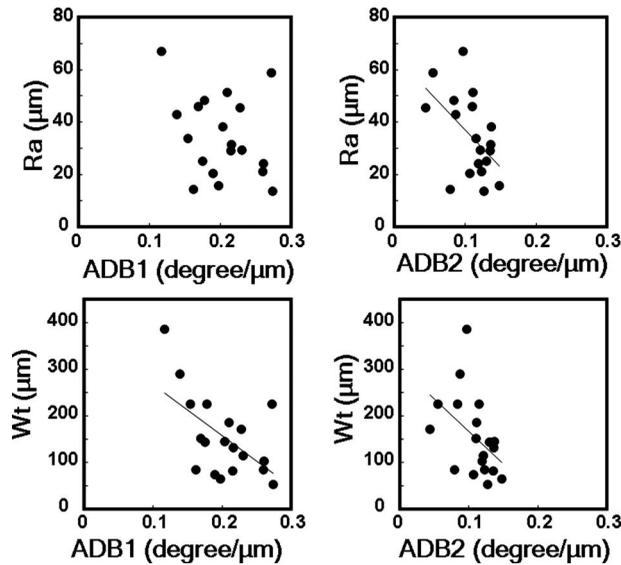
Fig. 7 Averaged dermal birefringence correlated with the parameters of skin roughness. Data were the same as that in Tables 1 and 2.

value in this study is almost the same as that in the previous study regarding the relationship between wrinkle score and Ra.[46] ADB2 showed a significant negative correlation with the depth and volume of the main horizontal wrinkle. These results suggest that the upper dermal degeneration of collagen and/or elastic fibers is related to the morphology of wrinkles. However, we could not detect the change of dermal birefringence localized in the parts of wrinkles. The result agrees with previous speculation for the mechanism of wrinkle formation. Kligman et al. reported that there was not any wrinkle-dependent histological dermal degeneration,[18] and photoaging-dependent dermal degeneration such as abnormality of elastic fibers brought decreased recuperative strength to deformation by external force during photoaging process, which promotes the progress of wrinkles. Bosset et al. also have the same opinion.[19] Tsuji speculated that the progress of abnormal elastic fibers accompanying photoaging promoted the deformation of the skin by external force and that the further progress of solar elastosis was influenced by the sun-exposed condition with the valley formation of wrinkles.[20,21] In either case, localized dermal degeneration may not be a direct factor to determine the generation of wrinkles. Meanwhile, the orientation of dermal birefringence may be related
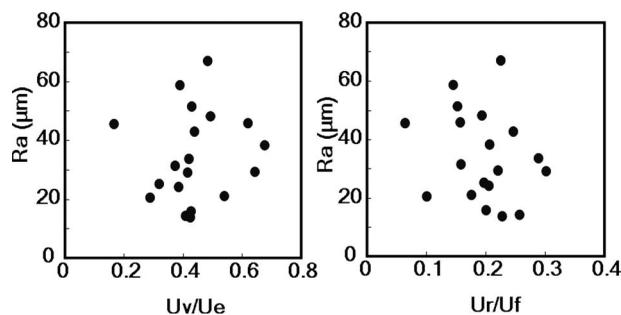
to wrinkling. A wrinkle in the eye-corner area progresses in the horizontal direction,[49] and the direction of the dermal fiber structure is thought to have an anisotropic property.[8,50,51] The orientation of dermal phase-retardation is another issue to be explored in the future.

Interestingly, there were depth-dependent correlations between averaged dermal birefringence and skin roughness parameters of the photoaged skin. Solar elastosis develops below the papillary dermis under the epidermis and does not have birefringence.[44] ADB2 may indicate the progress of solar elastosis under or in the papillary dermis. It may be reasonable to conclude that ADB2 correlates with the roughness parameters, such as Ra and Rz more than ADB1. Solar elastosis may be a major factor for the progress of wrinkles.

Alternatively, ADB1 correlated with Wt and Sm, but not Rz and Ra. Particularly, Sm means the spacing of grooves and showed a low correlation with Ra and Rz ($r = 0.477, 0.376$, respectively). The Grenz zone is a collagen-rich layer beneath the epidermis and is maintained even in elderly subjects.[10,52] Lavker demonstrated that the collagen fibrils in the upper Grenz zone are densely packed and highly oriented and contain fewer microfilaments.[53] Montagna et al., meanwhile, reported abundant small collagen fibers beneath the epidermis of photoaged skin.[54] The upper Grenz zone may be the result of some type of fibrotic change.[52,53] In this study, the subject with the deepest wrinkle had significantly high ADB1 and significantly low ADB2. The status of fibrosis in the Grenz zone may be influenced by factors other than photoaging. Alternatively, the Grenz zone is reported to contain degenerated collagen fibers. Nishimori et al. observed a dispersed collagen fiber structure in regions beneath the epidermis in photoaged skin.[15] Bernstein et al., meanwhile, noted differences in the collagen structure between the upper and lower parts of the Grenz zone.[14] At the least, depth-dependent dermal degeneration such as Grenz zone and solar elastosis may influence the skin morphology of photoaged skin in a different manner.

The parameters of skin elasticity measured by Cutometer did not correlate with the skin roughness. Skin elasticity decreases with aging,[28,29] and correlates with the roughness of photoaged skin across generations.[31] Moreover, sun-exposed sites decrease skin elasticity more than nonexposed ones.[44,29,33] Skin elasticity is thought to be a useful parameter to detect aging-dependent dermal degeneration. To our knowledge, however, there are no reports regarding the relationship between skin roughness and skin elasticity using subjects of the same generations. There were no relationships between skin elasticity and skin roughness parameters using only subjects in their seventies in this study. Cutometer measurment shows overall dermal degeneration, including intrinsic aging and photoaging.[28] PS-SD-OCT enables the measurement of only the upper dermis (100 to 300 μm), which is sensitive to photoaging, because we could not observe the change of dermal birefringence in the inner upper arm (nonexposed site) with aging in the previous study.[44] Moreover, the parameters of skin elasticity measured by Cutometer did not correlate with either of the averaged dermal birefringence data in this study (data not shown). The dermal birefringence is more sensitive to photoaging-specific dermal degeneration related to skin roughness than skin elasticity measured by Cutometer. Very recently, Fujimura et al. have reported that loss of skin

Fig. 8 The parameters of skin viscoelasticity did correlate with Ra, a skin roughness parameter. Data were the same as that in Table 2.

elasticity, measured by Cutometer, proceeds to increases of face wrinkle levels during aging.[32] They speculated that the amount of UV exposure to skin and not intrinsic aging was an direct factor to determine wrinkle levels.

In our previous study,[44] the region around the infundibulum of the hair follicle also showed a birefringence distinct from that of the regular dermis. This birefringence may disturb the quantification of the papillary and reticular dermal birefringence. It may be possible to raise the precision of the statistical analysis in the future by segmenting the birefringence around the infundibula.

In conclusion, the analysis of the upper dermal birefringence using PS-SD-OCT is useful not only to make a diagnosis of photoaged skin[44] but also to evaluate photoaging-dependent upper dermal degeneration related to skin roughness for the study of wrinkle formation. PS-SD-OCT is also expected to provide evidence for the efficacy test and mechanism study of antiwrinkle reagents.

Acknowledgments

References

1. S. Makki, J. C. Barbenel, and P. Agache, "A quantitative method for the assessment of the microtopography of human skin," *Acta Derm Venereol* **59**(4), 285–291 (1979).
2. J. L. Leveque, P. Corcuff, J. de Rigal, and P. Agache, "*In vivo* studies of the evolution of physical properties of the human skin with age," *Int. J. Dermatol.* **23**(5), 322–329 (1984).
3. E. Voros, C. Robert, and A. M. Robert, "Age-related changes of the human skin surface microrelief," *Gerontology* **36**(5–6), 276–285 (1990).
4. A. M. Kligman and R. M. Lavker, "Cutaneous aging: the differences between intrinsic aging and photoaging," *J. Cutan. Aging Cos. Dermatol.* **1**(1), 5–12 (1988).
5. J. Uitto, M. J. Fazio, and D. R. Olsen, "Molecular mechanisms of cutaneous aging. Age-associated connective tissue alterations in the dermis," *J. Am. Acad. Dermatol.* **21**, (3 Pt. 2), 614–622 (1989).
6. B. A. Gilchrest, "Skin aging and photoaging," *Dermatol. Nurs.* **2**(2), 79–82 (1990).
7. L. T. Smith, K. A. Holbrook, and P. H. Byers, "Structure of the dermal matrix during development and in the adult," *J. Invest. Dermatol.* **79**(Suppl. 1), 93S–104S (1982).
8. I. A. Brown, "Scanning electron microscopy of human dermal fibrous tissue," *J. Anat.* **113**(Pt. 2), 159–168 (1972).
9. S. Neerken, G. W. Lucassen, M. A. Bisschop, E. Lenderink, and T. A. Nuijs, "Characterization of age-related effects in human skin: a comparative study that applies confocal laser scanning microscopy and optical coherence tomography," *J. Biomed. Opt.* **9**(2), 274–281 (2004).
10. M. El-Domyati, S. Attia, F. Saleh, D. Brown, D. E. Birk, F. Gasparro, H. Ahmad, and J. Uitto, "Intrinsic aging vs. photoaging: a comparative histopathological, immunohistochemical, and ultrastructural study of skin," *Exp. Dermatol.* **11**(5), 398–405 (2002).
11. E. Schwartz, F. A. Cruickshank, C. C. Christensen, J. S. Perlish, and M. Lebwohl, "Collagen alterations in chronically sun-damaged human skin," *Photochem. Photobiol.* **58**(6), 841–844 (1993).
12. H. S. Talwar, C. E. Griffiths, G. J. Fisher, T. A. Hamilton, and J. J. Voorhees, "Reduced type I and type III procollagens in photodamaged adult human skin," *J. Invest. Dermatol.* **105**(2), 285–290 (1995).
13. J. H. Chung, J. Y. Seo, H. R. Choi, M. K. Lee, C. S. Youn, G. Rhie, K. H. Cho, K. H. Kim, K. C. Park, and H. C. Eun, "Modulation of skin collagen metabolism in aged and photoaged human skin *in vivo*," *J. Invest. Dermatol.* **117**(5), 1218–1224 (2001).
14. E. F. Bernstein, Y. Q. Chen, J. B. Kopp, L. Fisher, D. B. Brown, P. J. Hahn, F. A. Robey, J. Lakkakorpi, and J. Uitto, "Long-term sun exposure alters the collagen of the papillary dermis. Comparison of sun-protected and photoaged skin by northern analysis, immunohistochemical staining, and confocal laser scanning microscopy," *J. Am. Acad. Dermatol.* **34**(2 Pt. 1), 209–218 (1996).
15. Y. Nishimori, C. Edwards, A. Pearse, K. Matsumoto, M. Kawai, and R. Marks, "Degenerative alterations of dermal collagen fiber bundles in photodamaged human skin and UV-irradiated hairless mouse skin: possible effect on decreasing skin mechanical properties and appearance of wrinkles," *J. Invest. Dermatol.* **117**(6), 1458–1463 (2001).
16. G. J. Fisher, S. Kang, J. Varani, Z. Bata-Csorgo, Y. Wan, S. Datta, and J. J. Voorhees, "Mechanisms of photoaging and chronological skin aging," *Arch. Dermatol.* **138**(11), 1462–1470 (2002).
17. J. Y. Lee, Y. K. Kim, J. Y. Seo, C. W. Choi, J. S. Hwang, B. G. Lee, I. S. Chang, and J. H. Chung, "Loss of elastic fibers causes skin wrinkles in sun-damaged human skin," *J. Dermatol. Sci.* **15**, 15 (2008).
18. A. M. Kligman, P. Zheng, and R. M. Lavker, "The anatomy and pathogenesis of wrinkles," *Br. J. Dermatol.* **113**(1), 37–42 (1985).
19. S. Bosset, P. Barre, A. Chalon, R. Kurfurst, F. Bonte, P. Andre, P. Perrier, F. Disant, B. Le Varlet, and J. F. Nicolas, "Skin aging: clinical and histopathologic study of permanent and reducible wrinkles," *Eur. J. Dermatol.* **12**(3), 247–252 (2002).
20. T. Tsuji, T. Yorifuji, Y. Hayashi, and T. Hamada, "Light and scanning electron microscopic studies on wrinkles in aged persons' skin," *Br. J. Dermatol.* **114**(3), 329–335 (1986).
21. T. Tsuji, "Ultrastructure of deep wrinkles in the elderly," *J. Cutan Pathol.* **14**(3), 158–164 (1987).
22. J. L. Contet-Audonneau, C. Jeanmaire, and G. Pauly, "A histological study of human wrinkle structures: comparison between sun-exposed areas of the face, with or without wrinkles, and sun-protected areas," *Br. J. Dermatol.* **140**(6), 1038–1047 (1999).
23. L. H. Kligman, "The hairless mouse and photoaging," *Photochem. Photobiol.* **54**(6), 1109–1118 (1991).
24. K. Tsukahara, Y. Takema, T. Fujimura, S. Moriwaki, T. Kitahara, S. Imayama, and G. Imokawa, "All-trans retinoic acid promotes the repair of tortuosity of elastic fibres in rat skin," *Br. J. Dermatol.* **140**(6), 1048–1053 (1999).
25. S. Inomata, Y. Matsunaga, S. Amano, K. Takada, K. Kobayashi, M. Tsunenaga, T. Nishiyama, Y. Kohno, and M. Fukuda, "Possible involvement of gelatinases in basement membrane damage and wrinkle formation in chronically ultraviolet B-exposed hairless mouse," *J. Invest. Dermatol.* **120**(1), 128–134 (2003).
26. T. Sano, T. Kume, T. Fujimura, H. Kawada, S. Moriwaki, and Y. Takema, "The formation of wrinkles caused by transition of keratin intermediate filaments after repetitive UVB exposure," *Arch. Dermatol. Res.* **296**(8), 359–365 (2005).
27. C. Escoffier, J. de Rigal, A. Rochefort, R. Vasselet, J. L. Leveque, and P. G. Agache, "Age-related mechanical properties of human skin: an *in vivo* study," *J. Invest. Dermatol.* **93**(3), 353–357 (1989).
28. A. B. Cua, K. P. Wilhelm, and H. I. Maibach, "Elastic properties of human skin: relation to age, sex, and anatomical region," *Arch. Dermatol. Res.* **282**(5), 283–288 (1990).
29. Y. Takema, Y. Yorimoto, M. Kawai, and G. Imokawa, "Age-related changes in the elastic properties and thickness of human facial skin," *Br. J. Dermatol.* **131**(5), 641–648 (1994).
30. G. L. Grove, M. J. Grove, and J. J. Leyden, "Optical profilometry: an objective method for quantification of facial wrinkles," *J. Am. Acad. Dermatol.* **21**(3 Pt. 2), 631–637 (1989).
31. S. Akazaki, H. Nakagawa, H. Kazama, O. Osanai, M. Kawai, Y. Takema, and G. Imokawa, "Age-related changes in skin wrinkles assessed by a novel three-dimensional morphometric analysis," *Br. J. Dermatol.* **147**(4), 689–695 (2002).
32. T. Fujimura, K. Haketa, M. Hotta, and T. Kitahara, "Loss of skin elasticity precedes rapid increase of wrinkle levels," *J. Dermatol. Sci.* **47**(3), 233–239 (2007).
33. H. Adhoute, J. de Rigal, J. P. Marchand, Y. Privat, and J. L. Leveque, "Influence of age and sun exposure on the biophysical properties of the human skin: an *in vivo* study," *Photodermatol. Photoimmunol. Photomed.* **9**(3), 99–103 (1992).
34. S. Richard, J. de Rigal, O. de Lacharriere, E. Berardesca, and J. L. Leveque, "Noninvasive measurement of the effect of lifetime exposure to the sun on the aged skin," *Photodermatol. Photoimmunol. Photomed.* **10**(4), 164–169 (1994).

35. J. de Rigal, C. Escoffier, B. Querleux, B. Faivre, P. Agache, and J. L. Leveque, "Assessment of aging of the human skin by *in vivo* ultrasonic imaging," *J. Invest. Dermatol.* **93**(5), 621–625 (1989).

36. M. B. Quan, C. Edwards, and R. Marks, "Non-invasive *in vivo* techniques to differentiate photodamage and aging in human skin," *Acta Derm Venereol* **77**(6), 416–419 (1997).

37. H. K. Lee, Y. K. Seo, J. H. Baek, and J. S. Koh, "Comparison between ultrasonography (Dermascan C version 3) and transparency profilometry (Skin Visiometer SV600)," *Skin Res. Technol.* **14**(1), 8–12 (2008).

38. B. H. Park, C. Saxer, S. M. Srinivas, J. S. Nelson, and J. F. de Boer, "*In vivo* burn depth determination by high-speed fiber-based polarization sensitive optical coherence tomography," *J. Biomed. Opt.* **6**(4), 474–479 (2001).

39. M. C. Pierce, J. Strasswimmer, B. Hyle Park, B. Cense, and J. F. de Boer, "Birefringence measurements in human skin using polarization-sensitive optical coherence tomography," *J. Biomed. Opt.* **9**(2), 287–291 (2004).

40. M. C. Pierce, J. Strasswimmer, B. H. Park, B. Cense, and J. F. de Boer, "Advances in optical coherence tomography imaging for dermatology," *J. Invest. Dermatol.* **123**(3), 458–463 (2004).

41. M. C. Pierce, R. L. Sheridan, B. Hyle Park, B. Cense, and J. F. de Boer, "Collagen denaturation can be quantified in burned human skin using polarization-sensitive optical coherence tomography," *Burns* **30**(6), 511–517 (2004).

42. J. T. Oh, S. W. Lee, Y. S. Kim, K. B. Suhr, and B. M. Kim, "Quantification of the wound healing using polarization-sensitive optical coherence tomography," *J. Biomed. Opt.* **11**(4), 041124 (2006).

43. M. Yamanari, S. Makita, V. D. Madjarova, T. Yatagai, and Y. Yasuno, "Fiber-based polarization-sensitive Fourier domain optical coherence tomography using B-scan-oriented polarization modulation method," *Opt. Express* **14**(14), 6502–6515 (2006).

44. S. Sakai, M. Yamanari, A. Miyazawa, M. Matsumoto, N. Nakagawa, T. Sugawara, K. Kawabata, T. Yatagai, and Y. Yasuno, "*In vivo* three-dimensional birefringence analysis shows collagen differences between young and old photo-aged human skin," *J. Invest. Dermatol.* **128**(7), 1641–1647 (2008).

45. S. Jaspers, H. Hopermann, G. Sauermann, U. Hoppe, R. Lunderstädt, and J. Ennen, "Rapid *in vivo* measurement of the topography of human skin by active image triangulation using a digital micromirror device," *Skin Res. Technol.* **5**, 195–207 (1999).

46. T. Fujimura, K. Haketa, M. Hotta, and T. Kitahara, "Global and systematic demonstration for the practical usage of a direct *in vivo* measurement system to evaluate wrinkles," *Int. J. Cosmet. Sci.* **29**(6), 423–436 (2007).

47. M. Yamanari, M. Miura, S. Makita, T. Yatagai, and Y. Yasuno, "Phase retardation measurement of retinal nerve fiber layer by polarization-sensitive spectral-domain optical coherence tomography and scanning laser polarimetry," *J. Biomed. Opt.* **13**(1), 014013 (2008).

48. F. Kautzky, M. Dahm, M. Drosner, H. J. Vogt, and S. Borelli, "Direct profilometry of the skin: its reproducibility and variability," *J. Eur. Acad. Dermatol. Venereol.* **1995**(5), 15–23 (1995).

49. C. J. Kraissl, "The selection of appropriate lines for elective surgical incisions," *Plast. Reconstr. Surg.* **8**(1), 1–28 (1951).

50. M. D. Ridge and V. Wright, "The directional effects of skin. A bioengineering study of skin with particular reference to Langer's lines," *J. Invest. Dermatol.* **46**(4), 341–346 (1966).

51. G. E. Pierard and C. M. Lapiere, "Microanatomy of the dermis in relation to relaxed skin tension lines and Langer's lines," *Am. J. Dermatopathol.* **9**(3), 219–224 (1987).

52. M. Miyasaka, S. Sakai, A. Kusaka, Y. Endo, M. Kobayashi, K. Kobayashi, N. Hozumi, and R. Tanino, "Ultrasonic tissue characterization of photodamaged skin by scanning acoustic microscopy," *Tokai J. Exp. Clin. Med.* **30**(4), 217–225 (2005).

53. R. M. Lavker, "Structural alterations in exposed and unexposed aged skin," *J. Invest. Dermatol.* **73**(1), 59–66 (1979).

54. W. Montagna, S. Kirchner, and K. Carlisle, "Histology of sun-damaged human skin," *J. Am. Acad. Dermatol.* **21**(5 Pt. 1), 907–918 (1989).